

## Attenuation of High frequency P and S Waves in Qeshm Island, Iran

A. Zarean<sup>1</sup>, M. Farrokhi<sup>2</sup>, S. Chaychizadeh<sup>3</sup>

1. Geophysicists, Department of Geophysics, TOZco, Geological Survey of Iran, Tehran, Iran, Phone: +982188578648, Fax: +982188365524, Email: zarean@gmail.com
2. PhD. Student, Department of Seismology, International Institute of Earthquake Engineering and Seismology, Tehran, Iran, Email: moheba@yahoo.com
3. Ms. Student, Geophysics Institute, Tehran University, Tehran, Iran Phone: +989143062038, Fax: +982188365524, Email: sanazchaychizadeh@yahoo.com

### ABSTRACT :

Seismic waves attenuation of direct shear and P waves was investigated for the crust in Qeshm Island, the greatest Iranian Island in the Persian Gulf in north-western flank of the strait of Hormoz, using 100 seismograms of local earthquakes recorded after 2005 Qeshm earthquake. The data of a seismological network consisting of 17 stations, installed after the earthquake. We applied the single-station method (extended coda normalization method) to analyze  $Q_p^{-1}$  and  $Q_s^{-1}$  using the ratio of the P and S-wave to Coda-wave amplitude spectra, in the frequency range of 1.5 – 36 Hz, as a function of distance. The  $Q_p$  and  $Q_s$  is analyzed by using 66 lapse times of 22.5 – 87.5 seconds for center frequencies 1.5, 2, 3, 4, 5, 6, 7, 8, 9, 10, 11, 12, 14, 16, 18, 20, 24, 28, 32 and 36 Hz. The values of  $Q_p^{-1}$  and  $Q_s^{-1}$  estimated shows frequency dependence and decrease with increase of lapse time and distance indicates that the Q value increases with depth. The inverse of average of all quality factors for each frequency band is measured as  $Q_p^{-1}$  and  $Q_s^{-1}$ . The estimated  $Q_p^{-1}$  and  $Q_s^{-1}$  is highly frequency dependant and decrease from 0.07 and 0.06 in 1.5 Hz to 0.003 and 0.006 in 36 Hz, Respectively. Estimated  $Q_p^{-1}$  and  $Q_s^{-1}$  shows high frequency dependence with functional form  $0.06f^{-0.97}$  and  $0.1f^{-0.83}$ , respectively. The relatively low value of Q obtained in this study agrees with the value which is expected for a seismically active region such as Qeshm.

**KEYWORDS:** attenuation, coda normalization, Qeshm Island

## 1. IRODUCTION

Seismic wave's amplitude generally decreases with increasing travel distance through the earth. In infinite isotropic elastic media decrease of seismic waves is due to geometrical spreading, but in a real media like the earth seismic wave amplitudes decay with distance at a rate greater than predicted by geometric spreading. Several different approaches have been used to quantify the attention from different parts of seismograms e.g. Aki (1969), Aki and Chouet (1975), Mitchell (1995), each of which could be sensitive to different physical processes (e.g. an elastic absorption and scattering). An elastic absorption is affected due to some phenomena like grain defect, grain boundary, internal friction, sliding processes across cracks, and thermoelastic effects (Jackson and Anderson, 1974), and existence of heterogeneity in the crust cause scattering of seismic waves. Attenuation of seismic waves (an elastic absorption and scattering attenuation), expressed by the inverse of quality factor ( $Q^{-1}$ ). Quality factor is one of the most important geophysical parameters that shows similarity of media to an elastic media, (e.g. for an elastic media the quality factor will be infinite and for very dissipative media quality factor approach to zero). The value of  $Q^{-1}$  is particularly often used to predict strong ground motion for earthquake resistant construction design, and estimate of  $Q^{-1}$  is important in densely populated regions. Attenuation can be estimated using direct waves or coda waves. Aki (1969) proposed that appearance of coda waves caused by the incoherent waves scattered from random heterogeneity in the earth lithosphere. Aki and Chouet (1975) concluded that at low frequencies, less than 10 Hz, coda waves are dominated by scattered surface waves but at higher frequencies, coda waves are comprised mostly of scattered body waves as single backscattering s to s waves and they supposed zero distance of source receiver. Sato (1977) has extended the model to nonzero distances for two or three dimensional cases. Tsujiura (1978) showed that the site amplification determined for coda waves agreed well with that determined from direct S waves using the similarities and characteristics of coda waves and S waves, Aki (1980) proposed a single station method for measuring attention by normalizing direct S wave amplitude by S coda amplitude. This method accomplished by eliminating the influence of source and site effect so that attenuation can be isolated and studied in more details. Yoshimoto et al (1993) extended the conventional coda normalization method to measure  $Q_p^{-1}$ . Wu (1985) introduced Radiative transfer theory into seismology. According to radiative transfer theory, Aki (1992) concluded that coda waves are mainly composed of backscattering S-waves or conversion of P-wave to S-wave. zeng (1991), obtained an analytical solution describing the energy pattern vs. time and distance. Later, radiative transfer theory used to obtain the separate estimate of the scattering and intrinsic attenuation coefficient (Hoshiba, 1993). Using the uniform model, Fehler et al (1992) developed a method based on the analysis of the integrated energy vs. distance, calculated in three time window Analysis (MLTW) to separate scattering and intrinsic attenuation coefficient. The purpose of the present article is to estimate the S wave and P wave attenuation for different frequently using local earthquake data from the Qeshm Island, Iran. We used the single station method (coda Normalization method) based on the rate of decay of the S wave or P wave to coda wave amplitude ratio over distance for different frequencies. The same method has been applied by Aki (1980), Roecker et al (1982), Rebollar et al (1985), Yoshimoto et al (1993), Chung and Sato (2001), Kim et al (2004) to determined the attenuation of S wave attenuation and P wave attenuation for kanto region, Japan, South eastern Korea, and central South Korea. Finally a comparison is made between  $Q_p^{-1}$  and  $Q_s^{-1}$  values estimated in this study and other regions for frequencies between 1.5 and 36 Hz lapse time between 22.5 and 88.5 sec using single S to S backscattering model of Aki and Chouet (1975).

## 2. METHOD

We used coda normalization method (Aki, 1980) for estimation of  $Q_s^{-1}$  the method being designed to normalize the spectral amplitude of S waves by amplitude of coda waves at a constant lapse time. Aki (1969) analyses coda

waves and concluded that for earthquake with distances less than 200 Km and lapse time greater than twice S wave travel time, spectral amplitude of coda waves  $A_{ij}^S$  at lapse time  $T_c$  is independent of hypocentral distance and can be written as:

$$(1) \quad |A_{ij}^{Coda}(f)| \propto \frac{W_i^C(f)}{t_c^n} |N_j^C(f)|$$

Where  $f$  is frequency  $W_i^C$  is the source spectral amplitude of coda waves,  $N_j^C$  is site amplification of coda waves, and  $n$  is the effect of geometrical spreading. As Aki and Chout (1975), and Soto (1977) conclude that at lapse time greater than twice the S wave's travel time, source spectral amplitude of coda waves is proportional to source spectral amplitude of S waves ( $W_i^S(f)$ )

$$(2) \quad W_i^C(f) \propto g_0(f) W_i^S(f)$$

Where  $g_0(f)$  is total scattering coefficient. Spectral amplitude of direct S waves is:

$$(3) \quad |A_{ij}^{Direct-S}(f)|^2 \propto R_{\theta\phi} \frac{W_i^S(f)}{r_{ij}^2} |N_j^S(f)|^2 \exp\left(-Q_s^{-1}(f) \frac{2\pi f}{\beta} r_{ij}\right)$$

Where  $A_{ij}^{Direct-S}$  is spectral amplitude of S wave from  $i$ th earthquake recorded at  $j$ th station,  $N_j^S$  is site amplification of S waves,  $Q_s$  is quality factor of S waves,  $\beta$  is average velocity of S waves and  $R_{\theta\phi}$  is source radiation pattern. As Aki(1969), Aki and Chouet (1975), and Sato (1977), and Aki(1992) concluded that coda waves are the result of scattered waves from heterogeneous in the crust, and source effect of coda waves is similar to S waves. As tsujiura (1978), Aki (1980), Jin and Aki (1991), and Su et al (1992) concluded that site amplification of S waves and coda waves is similar. Aki(1980) using the properties of coda wave concluded that in order to normalize the source spectral amplitude of S wave ( $A_{ij}^S$ ) by the spectral amplitudes of coda waves  $A_{ij}^C$ , we divide (3) and (1):

$$(4) \quad \ln \frac{A_{ij}^{Direct-S}(f)}{A_{ij}^C(f)} = -\frac{\pi f}{Q_s(f)\alpha} r_{ij} + Const(f)$$

Using a data set from wide range of azimuths and data, the effect of radiation pattern can be neglected; we used equation (5) for estimation of  $Q_s^{-1}$  from a linear regression of left hand of equation (4) versus  $r$  by means of least square method. In this method because of the effects of coda waves the effect of source and site amplification can be neglected. For estimation of  $Q_p^{-1}$  we used the extended coda normalization method (Yoshimoto et al, 1993). Yoshimoto et al (1993) due to similarity of source spectral amplitude of P and S waves. For magnitudes less than 5, conclude that the coda normalization method can be used to estimate  $Q_p^{-1}$  as:

$$(5) \quad \ln \left[ \frac{A_{ij}^{Direct-P}(f)r_{ij}}{A_{ij}^C(f)} \right] = -\frac{\pi f}{Q_p(f)\alpha} r_{ij} + Const(f)$$

Where  $A_{ij}^{Direct-P}$  is spectral amplitude of P waves,  $Q_p$  is quality factor of P waves, and  $\alpha$  is average velocity of P waves. Using equation (5) we can estimate  $Q_p^{-1}$ . The extended coda normalization method can be used to estimate both  $Q_p^{-1}$  and  $Q_s^{-1}$ , simultaneously.

### 3. DATA

We collected three-component waveforms recorded at 17 stations of the Qeshm array (table 1). All of the stations are equipped with a broadband Guralp seismometer and Quanterra data logger with a 24-bit digitizer at 100samples/sec. The gain of a Guralp instrument is constant to ground velocity between 0.003 and 100 Hz.

Table 1 List of the coordinates of observation stations

Station Name	Signin map	Lat. (deg)	Long. (deg)	Geology
Airport	AIR	55,8920 E	26,7607 N	Quaternary Alluvium (Helucin)
Parvaz	PAR	55,8487 E	26,7625 N	Aghajari Formation (pelucein)
Gavarzin	GAVN	55,8268 E	26,7958 N	Quaternary Alluvium
Soheili	SOHE	55,7858 E	26,7565 N	Quaternary Alluvium
gas station	GAS	55,8583 E	26,8510 N	Aghajari Formation
Baghbala	BAGH	56,0315 E	26,8823 N	Quaternary Alluvium
Zeinabi	ZEIN	55,9570 E	26,8867 N	Aghajari Formation
zobe rooy	ZOBE	55,8735 E	26,8925 N	Aghajari Formation
Laft	LAFT	55,7565 E	26,8992 N	Aghajari Formation
Kaboli	KABO	56,2070 E	26,9545 N	Aghajari Formation
golenakhl	GOLE	56,0985 E	26,8553 N	Quaternary Alluvium
Rigou	RIGO	56,1243 E	26,8468 N	Quaternary Alluvium
Jijian	JIJN	56,0187 E	26,8455 N	Quaternary Alluvium
Suza	SUZA	56,0703 E	26,7820 N	Aghajari Formation
shotormorgh	SHOT	55,9852 E	26,8247 N	Quaternary Alluvium
Masen	MESE	56,0087 E	26,7438 N	Quaternary Alluvium
Shibderaz	SHIB	55,9310 E	26,6928 N	Aghajari Formation

We analyzed 1400 waveforms from 105 small events at Qeshm Seismic Network Stations. These events occurred from 1/12/2005 to 12/3/2006 with a range of magnitudes from 2 to 5.5 and a focal depth of less than 16 km. Station SUZA is located on Rock, whereas other stations are on different kinds of soil that are not known perfectly. Subsurface structure and near-surface velocity are uncertain, and only geological information such as rock types is available at each station. Figure 1 shows a distribution of stations. Figure 2 shows examples of three-component velocity seismograms observed at KABO.

Hypocentral distance of each events determined using a three layer with velocities 6, 6.5 and 8 km/s respectively for layer 1 (0-15 km), layer 2 (15-35 km) and a half space. Hypocentral distance determined by the difference of P and S-wave. For estimation of  $Q_s^{-1}$  distribution of hypocentral distance was less than 120 Km and for  $Q_p^{-1}$  was earthquakes from 40 to 160 km. Duration of time window of P, S, Coda waves and noise was 5 seconds. P-wave time window was starts from arrival of P wave to 5 seconds after it. S-wave time window was determined from arrival time of S wave to 5 seconds after it.

Spectral amplitude of S and P wave was determined by maximum amplitude of S-wave and P-wave window in a frequency band. Spectral amplitude of P-wave determined from vertical component and spectral amplitude of S-wave determined from both N-S and E-W.

Signal to noise ratio of P, S and Coda waves were 3, 4 and 2 respectively. We used a noise window start from beginning of seismogram to start of P-wave and amplitude of noise window determined by root mean square of noise window.

Amplitude of Coda waves determined by root mean square of Coda window centered at lapse time  $t_c$ . We used 66 lapse time (22.5 to 87.5 sec) greater than 1.5 to 2 times the S-wave arrival time to estimate  $Q_p^{-1}$  and  $Q_s^{-1}$  (Fig 2). We also used seismogram and envelope of seismogram. Envelope of seismogram determined by Hilbert transform of seismogram.



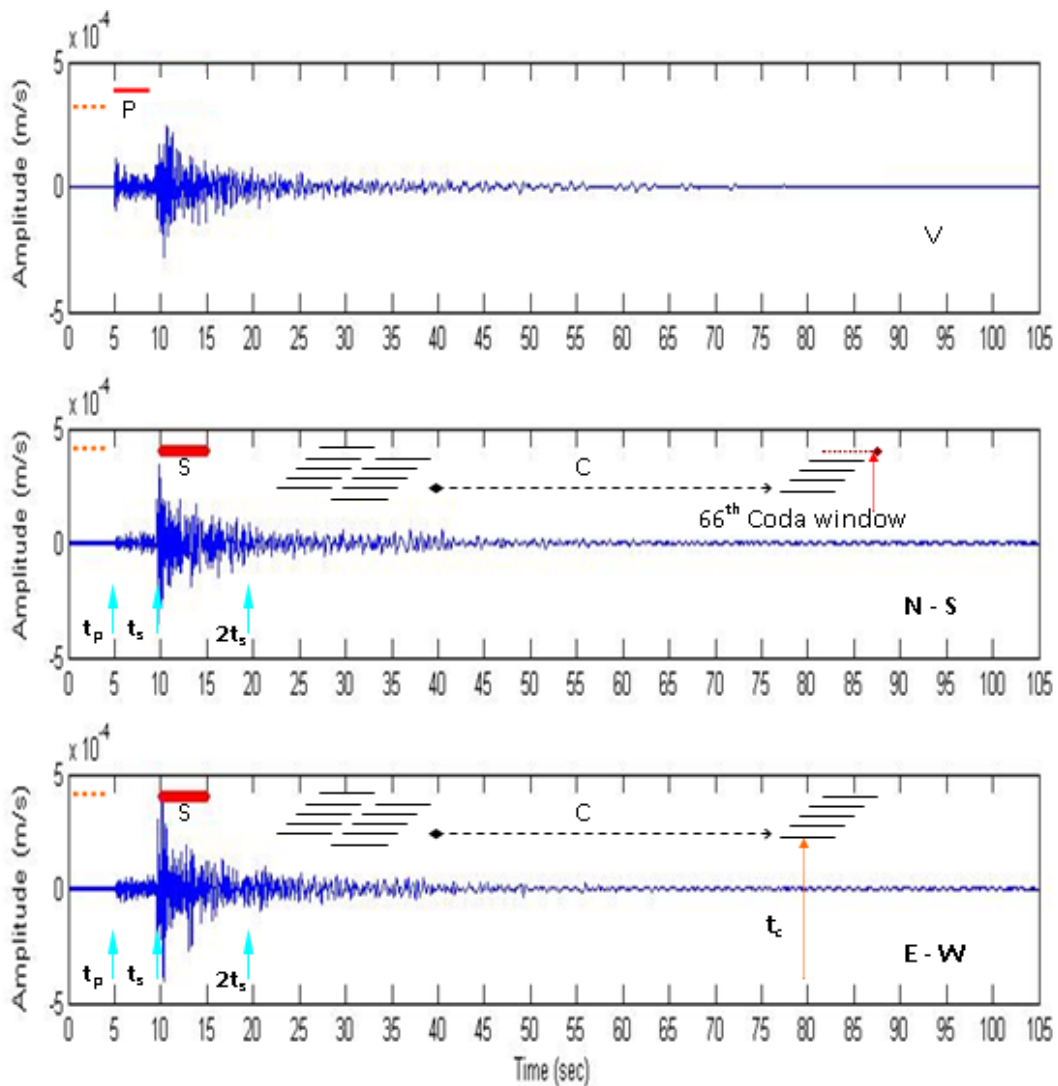


Figure 2 Seismogram recorded at KABO station. The horizontal bars shows the time windows used for the estimation of P, S, Coda waves and noise spectral amplitudes. The 66 Lapse time Coda wave windows used in this study to estimate quality factor is shown. Time is measured from origin time. P is P-waves, S is S-wave, C means Coda waves and N is noise window.  $t_p$ ,  $t_s$ , and  $t_c$  are arrival of P wave, S waves and center time of coda wave, respectively. V is vertical, N-S is north-south, and E-W is east-west component.

#### 4. MEASUREMENT OF $Q_p^{-1}$ AND $Q_s^{-1}$

From each velocity seismogram, we recorded a trend and baseline correction, then applied a cosine taper to both end of seismogram for a width of 10% of the full time window length. We used phaseless four-pole Butterworth filter with twenty octave width frequency bands from 1.5 to 36 Hz shown in table 2.

Table 2. Frequency band used in this study

center frequency (Hz)	1.5	2	3	4	5	6	7	8	9	10	11	12	14	16	18	20	24	28	32	36
BandWidth (Hz)	0.5	1	1	1	1	1	1	1	1	1	1	1	2	2	2	2	4	4	4	4

After we filter the seismogram and we calculate the envelope of it. Amplitude of P waves determined from maximum of P wave window from vertical component and envelope of that. The amplitude of S-wave determined separately. Coda wave window determined from each N-S E-W component and their envelope.

For estimation of  $Q_p^{-1}$  we use amplitude of P wave from vertical component and its envelope and Coda wave amplitude from N-S and E-W component and their envelope, respectively to normalize its amplitude. So we have estimated 4  $Q_p^{-1}$  for each lapse time and frequency band. For determining  $Q_s^{-1}$ , we used S-wave from both N-S and E-W component and their envelope, and calculate the ratio of S wave amplitude and Coda wave amplitude for each frequency and each lapse time, so we have 4  $Q_s^{-1}$  in each frequency band and lapse time. After normalization of P and S wave amplitude, we correct the ratio of direct wave to Coda waves for geometrical spreading, and then we had the left hand of equations (4) and (5), and used linear regression to determine the slope. With this assumption that  $V_s = 3.5$  km/s and  $V_p = 6$  km/s, we can determine  $Q_p^{-1}$  and  $Q_s^{-1}$  from the slope that calculated.

We neglect the negative  $Q_p^{-1}$  and  $Q_s^{-1}$ , and those quality factors that in their regression, R-square of regression becomes less than 0.1. Calculation for each of twenty frequency band and each component and their envelope was done. So we had nearly 66 values of  $Q_p^{-1}$  and  $Q_s^{-1}$  for each component, and we had that for two components and two envelopes.

The value of quality factor for each lapse time in a frequency band shows increase with increase of lapse time used, and it was because at higher lapse times, we had used the earthquake with greater hypocentral distances that in them waves penetrate to deeper layers with high quality factor.

Because of this aspect, for estimating the average quality factor of the area around the station we averaged the 66 values of  $Q_p^{-1}$  and  $Q_s^{-1}$  in each component, so for a value of quality factor in a frequency band, near the 264 value of quality factor for 66 lapse time and 4 components (two components and two envelopes) was used. Figure 4 shows the value of  $Q_p^{-1}$  and  $Q_s^{-1}$  in each station and average of them for Qeshm Island in our frequency range.

In frequencies that the signal to noise ratio of P, S and Coda waves were less than 3, 4 and 2 respectively, or for negative values of  $Q_p^{-1}$  and  $Q_s^{-1}$  or insufficient data, the value of  $Q_p^{-1}$  and  $Q_s^{-1}$  was not determined, so we could just determine quality factor for 13 stations.

As a result of our study, the decrease of average value of  $Q_p^{-1}$  and  $Q_s^{-1}$  in Qeshm Island from (0.07) and (0.06) at 1.5 Hz to (0.003) and (0.006) at 36 Hz. Values of  $Q_p^{-1}$  and  $Q_s^{-1}$  show strong frequency dependence, so we used a power law equation and determined the dependency of  $Q_p^{-1}$  and  $Q_s^{-1}$  in our seismic stations and average

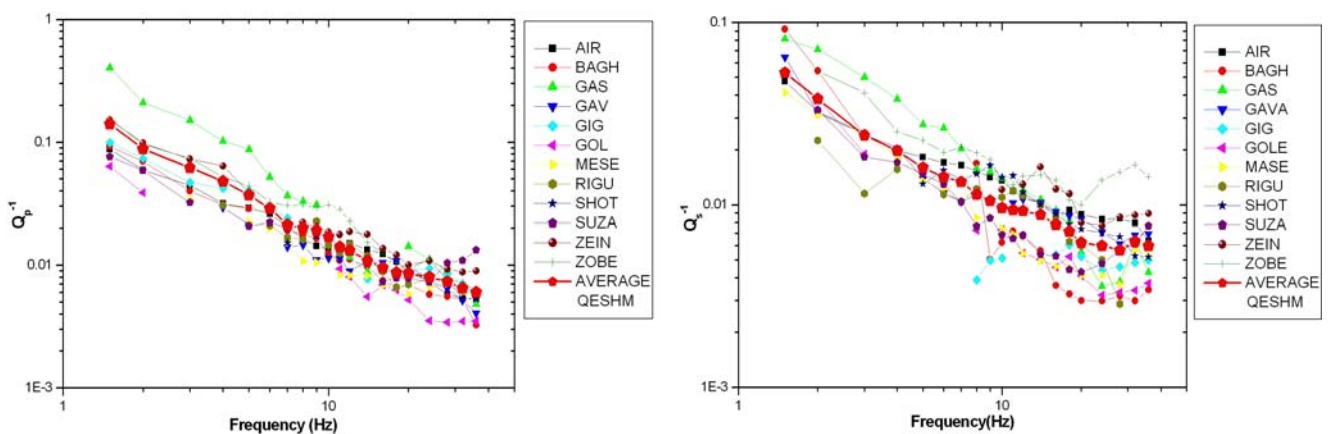


Figure 4 Value of  $Q_p^{-1}$  and  $Q_s^{-1}$  estimated in stations of Qeshm Seismic Network and average value of attenuation.

for Qeshm Island that shown in Table 3 Frequency dependence of average value of  $Q_p^{-1}$  and  $Q_s^{-1}$  in Qeshm Island calculated as  $(0.1)f^{(-0.83)}$  and  $(0.06)f^{(-0.97)}$ , respectively.

Table 3 Power law calculated for the estimated  $Q_p^{-1}$  and  $Q_s^{-1}$  in Qeshm Island and average of them.

Station	$Q_s^{-1}$	$Q_p^{-1}$
AIR	$0.055 f^{-0.64}$	$0.12 f^{-0.91}$
BAGH	$0.16 f^{-1.506}$	$0.14 f^{-1}$
GAS	$0.126 f^{-0.93}$	$0.07 f^{-1.46}$
GAV	$0.08 f^{-0.94}$	$0.07 f^{-0.7}$
GIG	$0.037 f^{-0.71}$	$0.4 f^{-0.89}$
GOLE	$0.08 f^{-1.1}$	$0.09 f^{-1}$
KABL	$0.01 f^{-0.48}$	$0.03 f^{-0.89}$
MASE	$0.06 f^{-0.88}$	$0.1 f^{-0.98}$
RIGU	$0.03 f^{-0.46}$	$0.09 f^{-0.8}$
SHOT	$0.04 f^{-0.5}$	$0.06 f^{-0.66}$
SUZA	$0.06 f^{-0.9}$	$0.11 f^{-0.96}$
ZEIN	$0.07 f^{-0.66}$	$0.22 f^{-1.04}$
ZOBE	$0.09 f^{-0.75}$	$0.22 f^{-0.98}$
AVERAGE	$0.06 f^{-0.97}$	$0.1 f^{-0.83}$

$Q_p^{-1}/Q_s^{-1}$  ratio for whole frequency band was greater than unity, which is similar to results of Yoshimoto et al (1993).

## 5. DISCUSSION

In fig. 5 we compare average value of  $Q_p^{-1}$  and  $Q_s^{-1}$  estimated for Qeshm Island with values from other of the world. We conclude that the high values of  $Q_p^{-1}$  and  $Q_s^{-1}$  of Qeshm are similar to estimated from Etna, and greater than other areas. High values of  $Q_p^{-1}$  and  $Q_s^{-1}$  in Qeshm Island may be the result of very complex lithosphere in this region under study, and high fractured area. Fig.4 showed the comparisons of values of  $Q_p^{-1}$  and  $Q_s^{-1}$  estimated for our seismic stations showed in table 1. As we understood, the value of  $Q_p^{-1}$  and  $Q_s^{-1}$  is maximum in Gavargin and zoberooy and is minimum in Golenakhl area. As shown by Vernant et al (2004) about the displacement in this area (little displacement) and historical earthquakes in this area. The low values of  $Q_p^{-1}$  and  $Q_s^{-1}$  may be due to cumulative energy in the crust of this area that might be released with a large earthquake. In this study we used the envelope of seismograms as well as seismograms, and our results of  $Q_p^{-1}$  and  $Q_s^{-1}$  showed little differences between the results of these two method. To estimate quality factor of P and S waves we used N-S and E-W component, and we saw that the results in E-W direction has little differences with those of the N-S component. These results are similar to results of Yoshimoto et al (1993).

For estimating  $Q_p^{-1}$  and  $Q_s^{-1}$  we used 66 lapse time from 22.5 to 87.5 second, and we saw that the value of  $Q_p^{-1}$  and  $Q_s^{-1}$  decreases with increase of lapse time, and its reason is in higher lapse times, we used earthquake with longer hypocentral distances and because of that the waves penetrates to deeper layers with high quality factor so the value of estimated  $Q_p^{-1}$  and  $Q_s^{-1}$  will decrease. Rebollar et al (1985) estimate quality factor in lapse time 10 and 16 seconds and saw that at longer lapse times the value of quality factor increases. Yoshimoto et al (1998) and Modiano and Hatzfeld (1982) using seismic events with hypocentral distances less than 40 km respectively in Nanganjo, Japan, and Arrete, France estimate high values for  $Q_p^{-1}$  and  $Q_s^{-1}$ . Also Campillo and Plantet (1991) using earthquakes with hypocentral distances between 200 and 1000 km estimated low values for  $Q_p^{-1}$ , and this shows increase of quality

factor with depth.

For frequencies greater than 1 Hz, as Yoshimoto et al (1993) concluded, the ratios of  $Q_p^{-1}/Q_s^{-1}$  estimated in this study was greater than unity. Aki (1992) using radiative transfer theory concluded that the conversion of S to P waves is more than the conversion of S to P when the wave hit the heterogeneity. amplitude of P wave decrease more than S waves because in heterogeneous media the converting P to S wave is dominant so amplitude of P wave decrease sharply and the  $Q_p^{-1}$  becomes greater than  $Q_s^{-1}$ , as a result of this, the ratio of  $Q_p^{-1}/Q_s^{-1}$  becomes greater than unity.

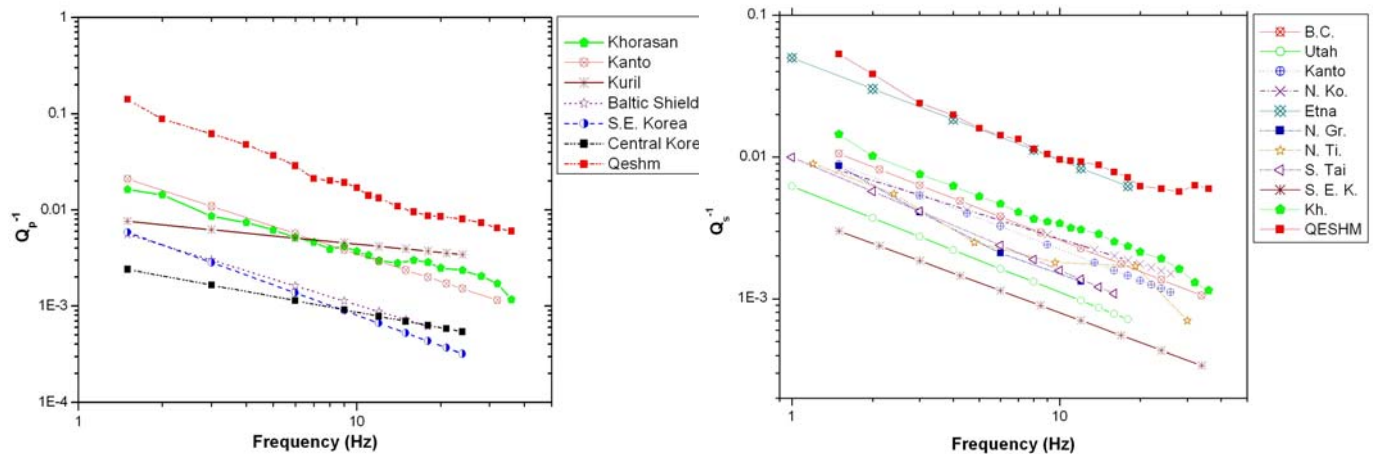


Figure 5 Comparison of estimated average  $Q_p^{-1}$  and  $Q_s^{-1}$  in Qeshm Island with other region of the world. In plot of  $Q_s^{-1}$  B.C. is Baja ,California (Rebollar et al, 1985), Utah (Jeon and Herman 1994), Kanto (Yoshimoto et al , 1993), N. Ko. is Northern Kogosima (Mamada and Takenaka, 2004), Etna (Del Pezzo et al, 1995), N. Gr. Is Northern Greece (Hatzidimitriou, 1995), N. Ti. is Northern Tien Shan (Martinov et al (1999), S. Tai. is Southwestern Taiwan (Chung and Kuang, 2006), S.E. Korea is South Eastern Korea (Kim et al, 2004), Kh. is  $Q_s^{-1}$  estimated in this study. For the plot of  $Q_p^{-1}$ , Kanto (Yoshimoto 1993), Kuril (Fedotov and Boldyrev, 1969), Baltic Shield (Kvamme and Havskov, 1989), S.E. Korea is South eastern Korea (Chung and Sato, 2001), and Central Koear (Kim et al, 2004).

## 6.CONCLUSION

High seismic risk and densely populated areas in Qeshm Island showed the need for seismic processing. Estimation of attenuation of seismic waves is an important issue in this approach. In this study we estimate the  $Q_p^{-1}$  and  $Q_s^{-1}$  values of seismic station of Qeshm Seismic Network.

In this study we estimate the average value of  $Q_p^{-1}$  and  $Q_s^{-1}$  for frequencies between 1.5 to 36 Hz, and saw that value of  $Q_p^{-1}$  and  $Q_s^{-1}$  decrease from 0.07 and 0.06 in 1.5 Hz to 0.003 and 0.006 in 36 Hz. Respectively.  $Q_p^{-1}$  and  $Q_s^{-1}$  values estimated in Qeshm Island were corresponding to those of seismically active regions. High values of  $Q_p^{-1}$  and  $Q_s^{-1}$  in Qeshm Island may be the result of very complex lithosphere in this region under study, and high fractured area. Qeshm Island has similarities with Etna area in seismology aspect.

## REFERENCES

- Aki, K. (1969). Analysis of the seismic coda of local earthquakes as scattered waves , J. Geophys. Res. 74, 615 – 631.
- Aki, K., and B. Chouet (1975). Origin of coda waves: Source, Attenuation, and scattering effects, J. Geophys. Res. 80, 3322 – 3342.
- Aki, K. (1980a). Attenuation of shear waves in the lithosphere for frequencies from .05 to 25 Hz, Phys. Earth Planet.

Inter. 21, 50 – 60.

Aki, K. (1992). Scattering conversions P to S versus S to P, *Bull. Seis. Soc. Am.* 82, 1969– 1972.

Berberian, M., and R. S. Yeets (1999). Patterns of Historical Earthquake Rupture in the Iranian Plateau, *Bull. Seis. Soc. Am.* 89, 120 -139.

Campillo, M., and J.L. Plantet (1991). Frequency dependence and spectral distribution of seismic attenuation in in France: experimental results and possible interpretations, *Phys. Earth Planet. Interiors.* 67, 48 – 64.

Chandra, U., J. G. Mcwhorter, and A. A. Nowroozi (1979). Attenuation of intensities in Iran, *Bull. Seis. Soc. Am.* 69, 237 – 250.

Chung, J. K. (2006). Prediction of Peak Ground Acceleration in Southwestern Taiwan as Revealed by Analysis of CHY Array Data, *TAO.* 17, 139 – 167.

Chung T. W. , H. Sato (2001a). Attenuation of high - frequency P and S waves in the crust of southeastern South Korea, *Bull. Seis. Soc. Am.* 91 , 1867 – 1874.

Del Pezzo, E., J. Ibanez, J. Morales, A. Akinci, and R. Maresca (1995). Measurements of Intrinsic and Scattering Seismic Attenuation in the Crust, *Bull. Seis. Soc. Am.* 85, 1373 – 1380.

Fehler , M., M. Hoshiaba, H. Sato, and K. Obara (1992). Separation of scattering and intrinsic attenuation for the Kanto-Tokai region, Japan, using measurements of S-wave energy versus hypocentral distance, *Geophys. J. Int.* 108, 787 – 800.

Fedotov, S.A., and S. A. Boldyrev (1969). Frequency dependence of the body wave absorption in the in the crust and the upper mantle of the kuril Islands chain. *Izv. Acad. Sci. USSR* 9, 17 – 33.

Fehler , M. , H. Sato (2003). Coda , *Pure. Appl. Geophys.* 160 , 541 – 554.

Hoshiaba, M. (1993). Separation of scattering attenuation and intrinsic absorption in Japan using the Multiple Lapse Time Window analysis of full seismogram envelope, *J. Geophys. Res.* 98, 15 808 – 15 824.

Jackson, D. D., and D. L. Anderson (1974). Physical mechanism of seismic-waves attenuation, *Review of Geophysics and space and space physics* 8, 1 – 63.

Jeon, Y. S., and R. B. Herrmann (2004). High-Frequency Earthquake Ground-Motion Scaling in Utah and Yellowstone, *Bull. Seis. Soc. Am.* 94, 1644 – 1657.

Kim K. D., T. W. Chung, and J. B. Kyung (2004). Attenuation of high - frequency P and S waves in the crust of Choongchung Islands, central South Korea, *Bull. Seis. Soc. Am.* 94, 1070 – 1078.

Kvamme, L. B., and J. Haskov(1989). Q in southern Norway, *Bull. Seis. Soc. Am.* 79, 1575 – 1588.

Mamada, Y., and H. Takenaka (2004). Strong Attenuation of Shear Waves in the Focal Region of the 1997 Northwestern Kagoshima Earthquakes, Japan, *Bull. Seis. Soc. Am.* 94, 464 – 478.

Martynov, V. G., F. L. Vernon, R. J. Mellors, and G. L. Pavlis (1999). High Frequency Attenuation in the Crust and Upper Mantle of the Northern Tien Shan, *Bull. Seis. Soc. Am.* 89, 215 – 238.

Mitchell, B. J. (1995). Anelastic structure and evolution of the continental crust and upper mantle from seismic surface wave attenuation, *Rev. Geophy.* 33, no. 4, 441–462.

Nuttli, O. W. (1980). The excitation and attenuation of seismic crustal phases in Iran, *Bull. Seis. Soc. Am.* 70, 469 – 485.

Rebollar, C. J., C. Traslosheros, and R. Alvarez (1985). Estimates of seismic wave attenuation in Northern Baja California, *Bull. Seis. Soc. Am.* 75, 1371 – 1382.

Roecker, S. W., B. Tucker, J. King, and D. Hatzfeld (1982). Estimates of Q in Central Asia as a function of frequency and depth using the Coda of locally recorded Earthquakes, *Bull. Seis. Soc. Am.* 72, 129 – 149.



- Sato, H. (1977a). Energy Propagation including scattering effects : Single isotropic scattering approximation, J. phys. Earth. 25, 27 -41.
- Sato, H. (1977b). Single isotropic scattering model including wave conversions: Simple theoretical model of the short period body wave propagations, J. Phys. Earth 25, 163 – 176.
- Sato, H., and M. Fehler (1998). Seismic wave propagation and scattering in the heterogeneous Earth ( AIP/Springer Verlag, New York 1998 ).
- Su, F., K. Aki, and N. Biswas (1991). Discriminating quarry blasts from earthquakes using coda waves, Bull. Seis. Soc. Am. 81, 162 – 178.
- Tsujiura, M. (1978). Spectral analysis of coda waves from local earthquakes, Bull. Earthquake Res. Inst. 53, 1 – 48.
- Vernant, Ph. et al., (2004a). Present-day crustal deformation and plate kinematics in the Middle East constrained by GPS measurements in Iran and Northern Oman, Geophys. J. Int., 157, 381–398.
- Yoshimoto, K., H. Sato, and M. Ohtake (1993). Frequency – dependence attenuation of P and S waves in the Kanto area, Japan, based on the coda normalization method, Geophys. J. Int. 114, 165 – 174.
- Yoshimoto, K., H. Sato, Y. Iio, H. Ito, T. Ohminato, and M. Ohtake (1998). Frequency-dependent attenuation of high-frequency P and S waves in the upper crust in western Nagano, Japan, Pure Appl. Geophys. 153, 489 – 502.